ELSEVIER

Polymer 42 (2001) 337–344

polymer

www.elsevier.nl/locate/polymer

Surface depth-profiling of polymer compounds using step-scan photoacoustic spectroscopy (S^2 PAS)

B.R. Kiland[a], M.W. Urban[a,*], R.A. Ryntz[b]

[a]*School of Polymers and High Performance Materials, The University of Southern Mississippi, Box 10076 Hattiesburg, MS 39406, USA*
[b]*Visteon Automotive Systems, Dearborn, MI 58121, USA*

Received 25 May 1999; received in revised form 19 December 1999; accepted 2 January 2000

Abstract

Depth-profiling of talc/polypropylene (PP) compounded polymers with 5, 10, 15 and 20% talc weight percents were examined to delineate concentration effects on surface stratification. This was achieved by utilizing step-scan photoacoustic spectroscopy (S^2 PAS) phase analysis to discriminate molecular concentration changes for each species across a distance of 9 μm from the sample surface. From phase analysis results, it was determined that not only does talc lie 1–2 μm closer to the surface than PP, but a layering effect results from an increase in talc concentration. This layering effect results in depths 0–3 μm becoming saturated with talc molecules at lower talc concentrations, and layers 3–9 μm showing evidence of saturation at higher concentrations. At these higher concentrations and greater depths, it is postulated that PP is displaced by talc molecules giving rise to a boundary layer consisting mostly of talc.

Keywords: Surface depth-profiling; Step-scan photacoustic spectroscopy; Thermoplastic olefins

1. Introduction

A polymer compound consists of a polymer species physically and often chemically modified by the incorporation of additives to optimize material properties. Properties modified include adhesion, stiffness, modulus, tensile strength and electrical properties by physically mixing organic by-products, metallic powders, minerals and other types of polymers. Injection-molded talc-filled polypropylene (PP) has replaced thermosetting polyesters in automotive applications due to the greater increase in mechanical properties. For example, a particular thermoplastic olefin (TPO) used frequently in the automotive industry consists of several components, such as PP, ethylene–propylene rubber (EPR), additives and fillers to optimize physical and chemical properties [1]. Talc, $Mg_3(OH)_2Si_4O_{10}$, is used as a reinforcement filler in TPO compounds, which not only improves the overall material properties, but is also responsible for increasing mechanical properties, enhancing surface quality, lowering mold shrinkage and improving compound processing as well [2].

The attributes of talc consist of excellent wetting and dispersing properties in polymers and a plate-like morphology. The weak van der Waals forces between talc particles allow the silicate layers to slide with relative ease in order to absorb stresses inflicted onto the compounded system. Aggregation of particles at the surface drastically reduces distribution and surface area, resulting in an overall reduction in properties.

Recently, we developed a photoacoustic (PA) phase analysis algorithm and applied the process to various systems to delineate component stratification at the surface [3]. These previous studies entailed time-dependent stratification processes, as well as processing-dependent processes. Essentially, the same concepts will be applied to this study, however, the effects of an increasing concentration of a particular component in an injection-molded sample will be determined by examining various concentrations of talc-filled PP samples.

2. Experimental

Injection-molded 2.5 mm thick talc/PP plaques consisting of 5, 10, 15 and 20% talc weight percentages were obtained from the Ford Motor Company. Talc [magnesium-silicate, $Mg_3(OH)_2Si_4O_{10}$] with an approximate particle size of 1.2 μm, used for a reference spectrum, was acquired from the Mallinckrodt Company and PP reference spectra were obtained using 2.5 mm thick plaques (Ford Motor Company).

* Corresponding author. Tel.: +1-601-266-6454; fax: +1-601-266-5635.
E-mail address: Marek.Urban@usm.edu (M.W. Urban).

0032-3861/01/$ - see front matter
PII: S0032-3861(00)00316-5

Table 1
Thermo-physical values used for talc/PP samples with various talc weight percentages

Talc (weight%)	κ (W/mK)	ρ (g/mL)	C_p (J/gK)
5	0.145	0.997	1.87
10	0.170	1.09	1.82
15	0.195	1.18	1.76
20	0.220	1.27	1.71

A Nicolet Magna-IR System 850 optical bench, purged with CO_2-free dry air and a He gas (99.999%) purged MTEC 100 photoacoustic cell was used for single-beam spectra acquisition. Step-scan experiments were performed using phase modulation of the IR light at an amplitude of two laser-fringe (1.266-μm retardation, or two He–Ne laser wavelengths, ^ $2\lambda_{He-Ne}$), at 632.8 nm retardation shift/step. Employing an analog-to-digital converter (ADC) allowed simultaneous acquisition of the I and Q signals at frequencies of 1000, 750, 400 and 300 Hz at 8 cm^{-1} resolution. Reference angles for each modulation frequency was determined using a 60% carbon black-filled elastomer (MTEC).

Phase analysis data processing included the use of Nicolet OMNIC E.S.P. 4.1a FT-IR software to acquire phase angle spectra, $\theta = \tan - 1(Q/I)$, and phase rotation spectra, $M(\phi) = I\cos(\phi) + Q\sin(\phi)$, where: ϕ is the projection angle. Thermo-physical values used for the various talc weight percentages are given in Table 1 [4,5].

3. Results and discussions

During injection-molding processing of a polymer compound, thermal and shear gradients result in an uneven distribution of various components at the surface [1,6,7]. This material processing involves filling a molten polymer into a mold, where high-pressure packing followed by a cooling stage produces the final product. Two of the most important stages of this process, which determine the rheological properties of the final polymer, are the filling and cooling stages. During the filling stage, the visco-elasticity of the polymer results in elastic and shear deformations, whereas polymer relaxation occurs in the cooling stage [8]. Consequently, both stages effect molecular orientations within the final molded part, thereby perturbing morphology near the surface, which influences final properties such as cohesion, adhesion, and overall performance [9,10]. While processing gradients cause component separation, various surface energies and physical properties of the materials used in a compounded sample may produce a layered surface as well.

A number of surface sensitive techniques have been applied previously to various systems; however, few offer the nondestructive capabilities of photoacoustic spectroscopy (PAS) [11–23]. PAS offers several unique attributes, such as surface analysis and depth-profiling capabilities. Utilizing these advantages, step-scan photoacoustic spectroscopy (S^2 PAS) was selected as the method for depth profiling compounded talc/PP samples with various talc weight percentages. In particular, monitoring of PA signal phase, or the finite time length between signal generation and detection, provides more coherent and complete surface analyses. With this spectroscopic method, we intend on determining talc and PP absorbing layer depths, and surface concentration changes as a function of these component concentrations.

Fig. 1 illustrates the individual PA single-beam spectra of PP (trace A) and talc (trace B), showing bands within the wavenumber range of 1500–600 cm^{-1}. Figs. 2 and 3, acquired at a modulation frequency of 400 Hz, present single-beam (traces A) and phase angle spectra (traces B) for the lower (5%) and upper (20%) talc weight percentages used for the analysis. As shown in these figures, several unique contributions for each component exists within this spectral range of 1550–900 cm^{-1}, which are listed in Table 2. For example, the band located at 1378 cm^{-1} (CH_3

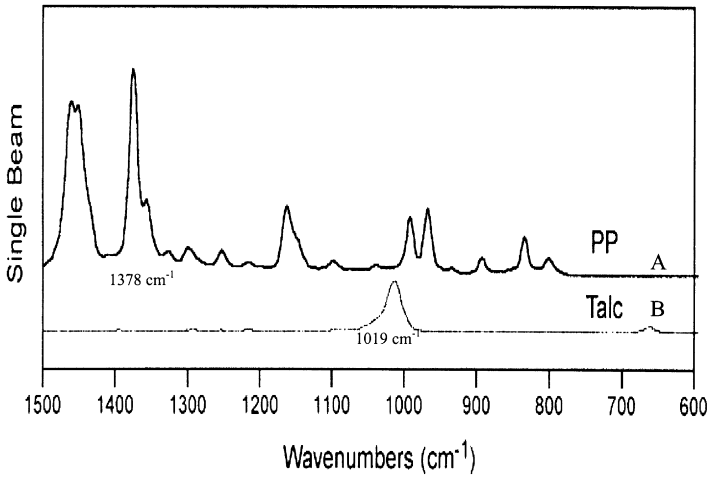

Fig. 1. PA FT-IR spectra of (A) PP and (B) talc showing the bands at 1378 and 1019 cm^{-1} for PP and talc, respectively.

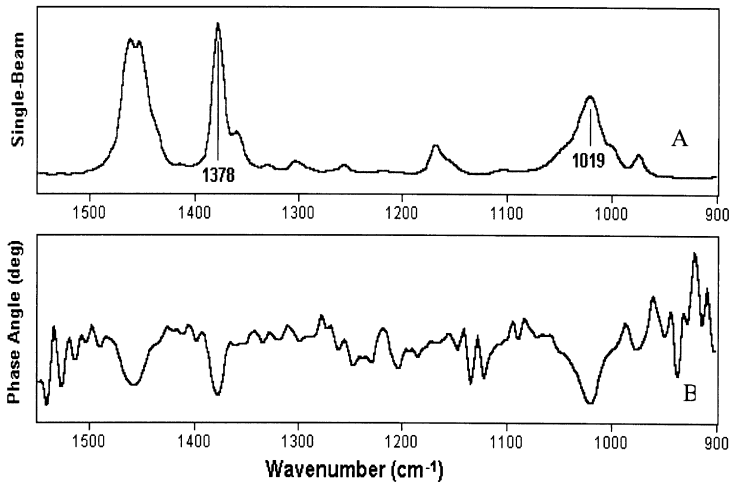

Fig. 2. Single-beam (A) and phase spectra (B) of a 5% (weight percent talc) sample obtained at 400 Hz within wavenumbers 1550–900 cm^{-1}.

deformation + CH_2 wagging + C–C chain wagging) results from PP vibrations, and the band positioned at 1019 cm^{-1} (Si–O stretching) corresponds to silicate contributions of talc in the compounded sample. Since marginal band overlap exists between species at these wavenumbers, the bands at 1378 and 1019 cm^{-1} were selected for depth-profiling analysis. A tentative IR band assignment table, including the associated absorbing components for the spectral range of 1550–900 cm^{-1} is given in Table 2.

Besides an obvious increase in the band at 1019 cm^{-1} due to a higher talc concentration, a feature distinguishing Fig. 3 from that shown in Fig. 2, is evident from a comparison of PP and talc phase spectra. By increasing the talc concentration from 5 to 20%, the difference between phase values of the bands at 1019 and 1378 cm^{-1} increases. This effect may be interpreted as either a shorter time delay between signal generation and detection for talc, or a longer time with respect to PP, as talc concentration increases. In essence, the larger difference suggests the existence of migratory tendencies of talc toward the surface, coupled with the traversing of PP further into the bulk of the sample, or the separation of layers with increasing talc concentration. Our previous stratification studies have shown analogous results for compounded TPO samples, which are similar to the talc/PP system in terms of sample processing, but compositionally differ by the presence of a rubber elastomer [3,24]. Studies performed on TPO samples by other authors suggests that component incompatibility produces discrete boundary layers consisting of various lamellae of homogenous materials near the surface [1,8]. Since the constituents of both systems are similar, the talc/PP system may produce corresponding results with respect to TPO.

A further examination of this phase angle dependence on concentration was performed by analyzing the phase spectra, similar to Figs. 2 and 3 of samples with 5, 10, 15 and 20% talc weight percent. As shown in previous studies, a phase shift correction must be applied to experimental data acquired at different frequencies in order to obtain accurate PA signal depths [3]. This phase shift correction takes into account the frequency dependence of the collection angle,

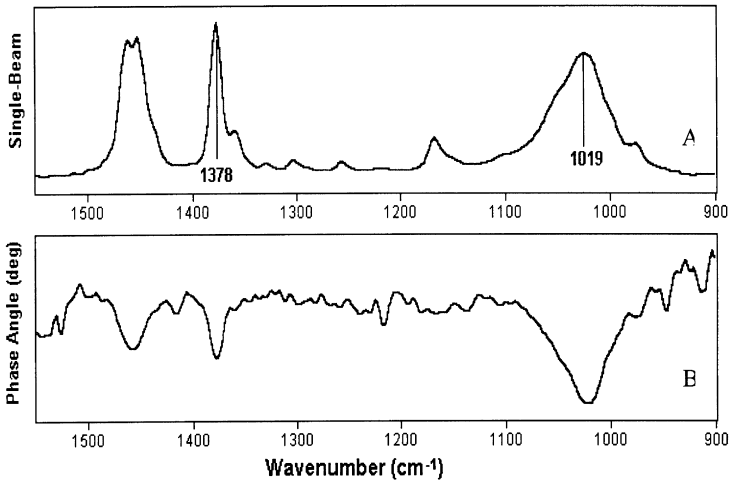

Fig. 3. Single-beam (A) and phase spectra (B) of a 20% (weight percent talc) sample obtained at 400 Hz within wavenumbers 1550–900 cm^{-1}.

Table 2
Tentative band assignment table for talc/PP compounded system for the wavenumber range of 1550–900 cm^{-1} (ν = stretching, ρ = rocking, δ = deformation, ω = wagging, τ = twisting

Wavenumber (cm^{-1})	Component	Assignment
1462	PP	$\delta(-CH_3)$
1453	PP	$\delta(-CH_2) + \delta(CH_3)$
1378	PP	$\delta(-CH_3) + \omega(-CH_2) + \omega(C-C)$
1358	PP	$\delta(-CH) + \nu(C-C) + \omega(-CH_2)$
1302	PP	$\omega(-CH_2) + \tau(-CH_2) + \delta(-CH)$
1261	PP	$\delta(-CH) + \tau(-CH_2) + \rho(-CH_3)$
1168	PP	$\nu(C-C) + \delta(-CH) + \rho(-CH_3)$
1045	PP	$\nu(C-CH_3) + \nu(C-C) + \delta(CH)$
1019	Talc	$\nu(Si-O)$
999	PP	$\delta(-CH) + \rho(C-C) + \omega(C-CH_3)$
972	PP	$\rho(CH_3) + \omega(C-C)$

and has been proven useful for similar stratified systems [3]. Curves A–D in Fig. 4 show the phase angles for the 1019 cm^{-1} Si–O stretching band of talc plotted as a function of modulation frequency for samples with talc percentages of 5, 10, 15 and 20%, respectively. As demonstrated in this figure, the phase angles decrease as talc concentration increases from 5 to 20%, or, likewise, PP concentration decreases. However, a much greater phase angle difference is observed as talc concentration increases from 5–15%, in comparison to the 15 and 20% trace differences. In order to compare these results with PP phase behavior, a similar plot was constructed for the PP band at 1378 cm^{-1} (Fig. 5), which depicts an opposite trend. In contrast to Fig. 4, two phase angle behaviors of PP detection are shown as talc concentration increases, or alternatively as PP concentration decreases. The first behavior concerns the high frequencies, where an increase in phase angle occurs as the talc concentration is increased. An opposite effect results at the lowest frequencies, which display a decrease in phase angle as talc concentration increases. Another noticeable difference between Figs. 4 and 5 concerns the smaller difference in phase angle values as talc concentration is increased.

One of the advantages performing PA phase analysis is the ability to determine signal depth, x, from phase spectra measurements [25–30]. Using an equation relating phase angle and PA signal origin, $x = \theta'\mu$, (where θ' is the corrected phase angle) frequency dependent depths for both talc (Fig. 6) and PP (Fig. 7) were calculated. Table 3 lists the actual depth values for the various concentrations studied at experimental frequencies of 1000, 750, 400 and 300 Hz. Examining the graph showing the talc distribution curves in Fig. 6, an effect similar to that found in Fig. 4 is observed: a wide distribution difference occurs between the traces for 5–15% talc concentration, along with a much smaller difference in depth between the 15–20% traces. More specifically, the widest distributions exist at depths approximately 3–6 μm from the surface. Within these distances, the large decrease in PA signal depth as talc concentration is increased may be attributed to talc migration toward the surface, occurring up to a critical concentration somewhere between 15–20% weight percent talc. At these concentrations, a noticeably smaller change in depth occurs for frequencies within 300–1000 Hz.

A different trend is shown in the PP distribution curves as talc concentration is increased. Illustrated in Fig. 7, PP traces display a significant change in absorbing layer depth between 3–5 μm, showing PP migration away from the surface as talc concentration increases. This result offers further support of the theory that the largest migration of talc occurs at approximately 3–6 μm. However, in this case the detection of PP molecules further from the surface may be a result of talc displacing PP within this layer at higher talc concentrations.

Plot of the surface depth as a function of talc% w/w, such as shown in Fig. 8 (traces A–H) allows us to analyze talc and PP distribution patterns as a function of concentration. As illustrated in this figure, talc approaches the surface as

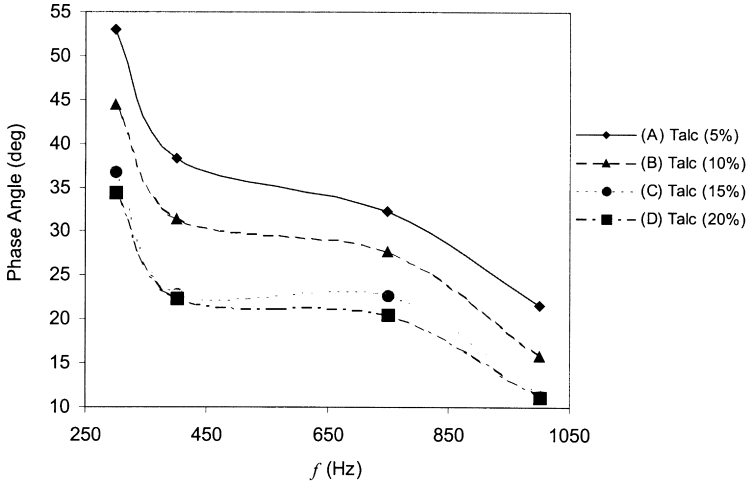

Fig. 4. Plot showing corrected PA phase angles, θ', versus modulation frequency, f, for the talc band at 1019 cm^{-1}. Each trace represents samples with talc weight percentages of (A) 5%, (B) 10%, (C) 15% and (D) 20%.

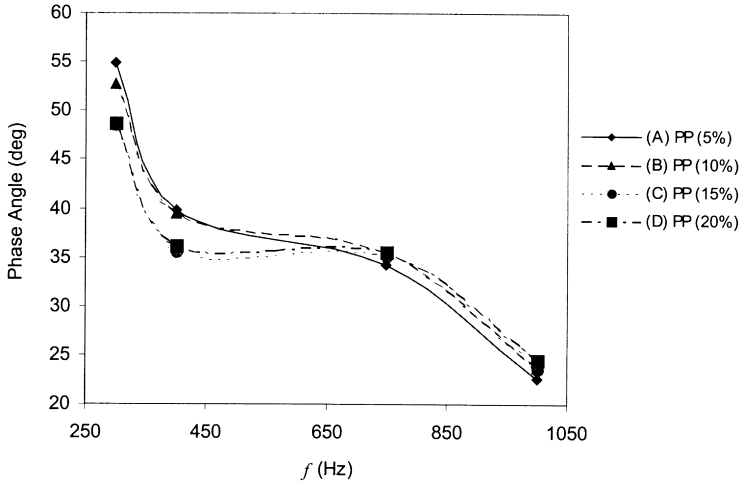

Fig. 5. Plot showing corrected PA phase angles, θ', versus modulation frequency, f, for the PP band at 1378 cm^{-1}. Each trace represents samples with talc weight percentages of (A) 5%, (B) 10%, (C) 15% and (D) 20%.

the weight percentage increases. However, for depths greater than 4 μm from the surface, the trace patterns of PP decrease in depth as talc concentration changes from 10 to 15%, followed by a depth increase as talc concentration is increased to 20%. This effect may be a result of a critical concentration experienced by layers near the surface at approximately 15%, where aggregation of particles at the surface may pack most efficiently. Beyond this point, talc packs less efficiently within 0–4 μm, and talc begins displacing the PP molecule at depths greater than 4 μm. In addition, other authors have observed this phenomena ascribing it to low molecular weight amorphous PP traveling toward the surface during the cooling stage of processing [1]. Therefore, the possibility of the 15% sample having a relatively higher abundance of low molecular weight PP, than the 10 and 20% samples exists.

Further evidence supporting the above theories can be shown by monitoring the change in talc concentration with depth, or by plotting the derivative of the phase rotation magnitude of each band with depth, $\Delta M'/\Delta x$ versus x, shown in Fig. 9 [3]. This is performed by rotating the I and Q spectra to the phase angle, which maximizes the rotation magnitude. For illustrative purposes, division of the traces into three into three layers (I–III), spaced 3 μm apart, allows us to determine the stratification of components as talc concentration is increased. Layer I (0–3 μm) shows large changes in talc concentrations going from

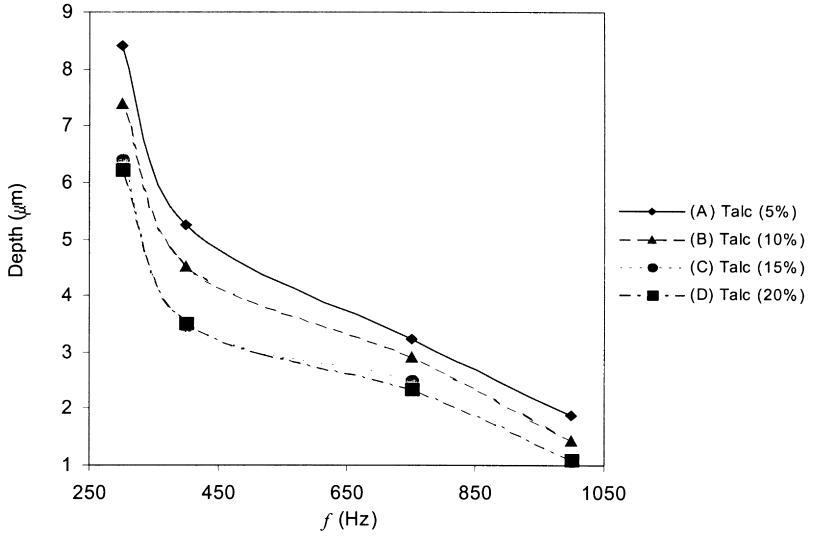

Fig. 6. PA signal depth versus modulation frequency, f, for the talc band at 1019 cm^{-1}. Traces A–D represent data for samples with talc weight percentages of 5, 10, 15 and 20%, respectively.

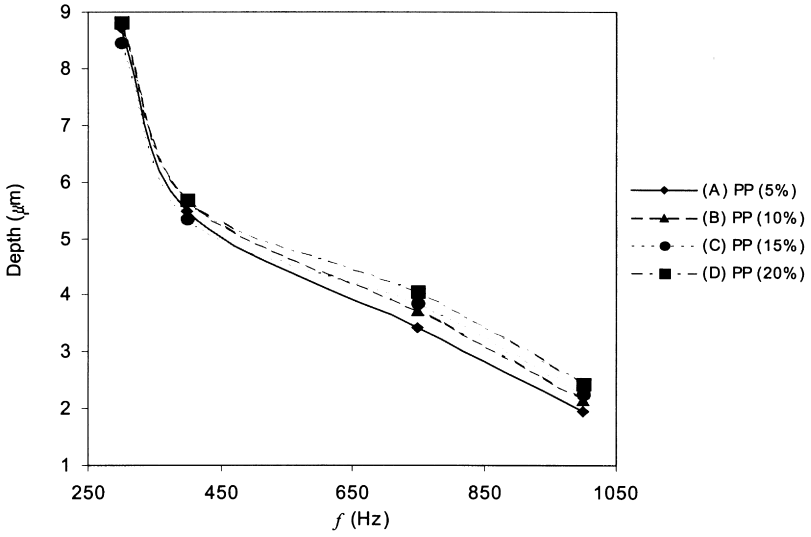

Fig. 7. PA signal depth versus modulation frequencies, *f*, for the PP band at 1378 cm^{-1}. Traces A–D represent data for samples with 0 talc weight percentages of 5, 10, 15 and 20%, respectively.

5–15%, followed by a marginal increase as the concentration is increased to 20%. In contrast, layer II (3–6 μm) shows significantly large increases in talc concentration, and, most noticeably, as talc concentration is increased from 15 to 20%, a larger increase in signal occurs. This supports the notion that within 0–3 the particles reach a critical concentration, where a decrease in migration results due to this layer being saturated with talc. Once layer I is saturated with talc molecules, migration occurs to a greater extent within the adjacent layer (3–6 μm). The concentration decreases into layer III (6–9 μm), where even less talc molecules are present.

Table 3
Corrected phase angles, θ' and calculated depths of talc/PP samples with talc weight percentages of 5, 10, 15 and 20%

Talc (weight%)	*f* (Hz)	PP depth		Talc depth	
		PP θ' (°)	(μm)	Talc θ' (°)	(μm)
5	1000	22.6	1.96	21.6	1.88
10		23.8	2.17	15.9	1.45
15		23.6	2.25	11.3	1.08
20		24.6	2.44	11.1	1.10
5	750	34.2	3.43	32.3	3.24
10		35.5	3.74	27.7	2.92
15		35.1	3.87	22.7	2.50
20		35.5	4.06	20.5	2.35
5	400	39.8	5.46	38.2	5.25
10		39.5	5.69	31.4	4.53
15		35.5	5.36	23.0	3.46
20		36.2	5.67	22.4	3.51
5	300	54.9	8.70	53.0	8.40
10		52.8	8.79	44.5	7.41
15		48.5	8.45	36.8	6.42
20		48.7	8.81	34.4	6.23

Notice also that talc concentration appears to be more evenly distributed at lower concentrations.

If one applies the same principles to the PP band at 1378 cm^{-1}, a significantly more complex situation exists which is illustrated in Fig. 10. Layer I (0–3 μm) indicates that an increase in talc concentration at the surface results not only in detection of PP further from the surface, but also a decrease in concentration change with depth is observed. Layer II (3–6 μm) demonstrates a similar behavior as Fig. 8, showing the detection of PP further into the sample for the 10% than the 15% sample. Examination of the 15 and 20% traces indicates the presence of PP closer to the surface for the 15% talc weight percent sample within layer II, in addition to a larger change in concentration with depth. Relating this effect with the results from Fig. 9, if a net migration of talc occurs after 15% within layer II, PP concentration should decrease as the talc molecules displace PP molecules at the 20% concentration. Furthermore, if this effect is coupled with the presence of a higher content of low molecular weight amorphous PP in the 15% compared to the other samples, the same results should occur to a greater extent. These data demonstrate that stratification of individual TPO components indeed occurs and its origin most likely results from the flow and heterogeneous characteristics of TPO components. An approximately 1.2 μm in diameter talc particle can act as the nucleating agent for PP crystallization, and at the same time, PP being more crystalline than the EP, will exhibit lower flow rates and lower viscosity at given shear rates and temperatures. As a result, PP will move to the flow front during the injection molding process, thus crystallizing with access of talc near the mold surface.

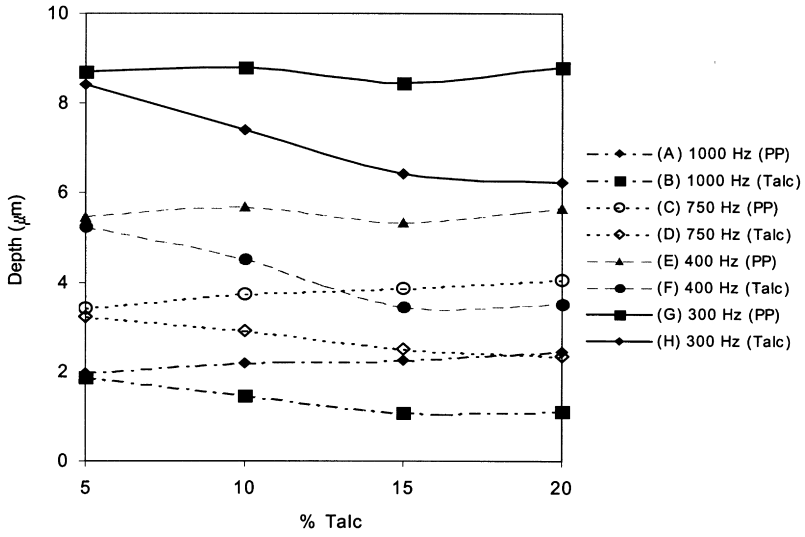

Fig. 8. PA signal depth (μm) of 1378 and 1019 cm^{-1} band plotted as a function of weight percent talc for modulation frequencies of 1000 (A, B), 750 (C, D), 400 (E, F) and 300 Hz (G, H).

4. Conclusions

Monitoring the phase values of the PA signal, the effects of increasing the talc concentration within a talc/PP injection-molded sample has been determined and based on a previously developed S^2 PAS phase analysis theory, depth-profiling of talc and PP for samples with various talc concentrations were probed. From analysis of phase spectra data, large decreases in absorbing layer depth for talc were observed as a function of concentration. At shallow depths (0–3 μm) the change in talc concentration appeared to increase to a limited extent after reaching a talc weight percent of 15%. Conversely, PP exhibited a decrease in absorbing layer depth, as well as a reduction in concentration change at distances of 0–3 μm. In contrast, the most significant changes in talc concentration were observed at distances 3–6 μm from the surface, possibly due to a high talc concentration at the shallower depths, in addition to the migration of talc into this layer. Within this same layer, PP decreases in a similar manner as compared to depths ranging from 0–3 μm. In contrast, a smaller change in PP concentration is detected for a talc weight percent of 20% in comparison to the 15% sample. These data suggest that talc has a greater tendency to migrate toward the surface, as compared to PP, in addition to the fact that after a value of 15%, the saturation of talc occurs within 0–3 μm. Beyond this concentration, the amount of talc increases at a higher rate at depths below this layer, and the displacement PP results.

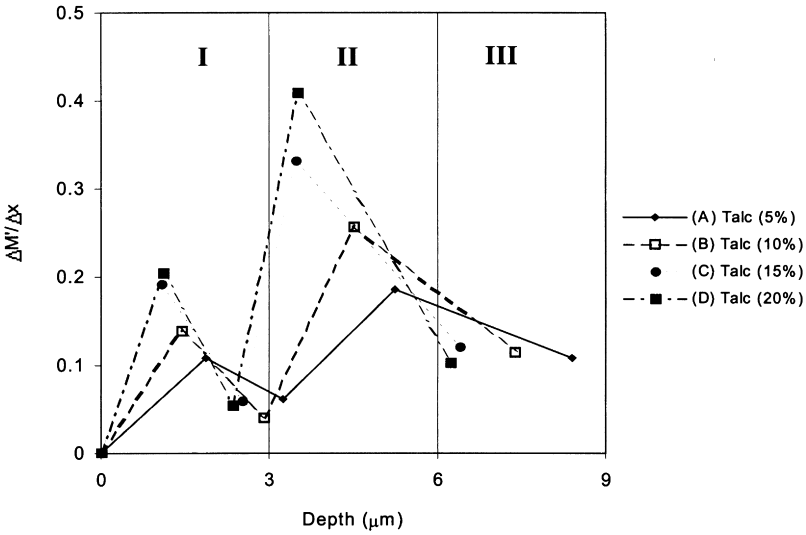

Fig. 9. Plot of the rotation magnitude derivative, $\Delta M'/\Delta x$, with respect to distance, x (μm), for the 1019 cm^{-1} band for samples with talc weight percentages of (A) 5%, (B) 10%, (C) 15% and (D) 20%.

References

[1] Ryntz RA. Prog Org Coat 1996;27:241.
[2] Katz HS, Milewski JV. Handbook of fillers for plastics. New York: VAN Nostrand Reinhold, 1987.
[3] Kiland BR, Urban MW. North Dakota State University, unpublished results.
[4] Touloukina YS, Powell RW, Ho CY, Nicolaou MC. Thermophysical properties of high temperature solid materials, vol. 6. New York: Macmillan, 1967.
[5] Hall C. Polymer materials. New York: Wiley, 1981.
[6] Fitchmun DR, Mencik Z. J Polym Sci: Polym Phys Ed 1973;11:951.
[7] Kantz MR, Newman HD. J Appl Polym Sci 1972;16:1249.
[8] Ryntz RA, Qie X, Ramamurthy AC. The Effects of Coating Solvents On the Morphology of Thermoplastic Olefins, Ann. Waterborne, Higher-Solids, and Powder Coatings Symp. Feb. 11, 1994, New Orleans, LA.
[9] Tadmor Z. J Appl Polym Sci 1974;18:1753.
[10] Flaman AA. Polym Engng Sci 1993;33:193.
[11] Thorstenson TA, Urban MW. J Appl Polym Sci 1993;47:1381.
[12] Thorstenson TA, Urban MW. J Appl Polym Sci 1993;47:1387.
[13] McDonald WF, Urban MW. J Adhes Sci Technol 1990;4:751.
[14] Salazar-Rojas EM, Urban MW. Prog Org Coat 1989;16:371.
[15] Niu BJ, Urban MW. J Appl Polym Sci 1995;56:377.
[16] Harthcock MA, Atkin SC. J Appl Spectrosc 1988;42:449.
[17] Weyher JL, Van de Ven J. J Cryst Growth 1987;78:191.
[18] Ludwig BW, Urban MW. J Coat Technol 1994;66:59.
[19] Ludwig BW, Urban MW. Polymer 1994;35:5130.
[20] Niu BJ, Urban MW. J Appl Polym Sci 1996;62:1903.
[21] Niu BJ, Urban MW. J Appl Polym Sci 1996;60:389.
[22] Evanson KW, Urban MW. J Appl Polym Sci 1991;42:2297.
[23] Kim H, Urban MW. Langmuir 2000;16(12):5382–90.
[24] Pennington BD, Urban MW, Ryntz RA. Polymer 1999;40:4795.
[25] Jiang EY, Plamer RA. J Appl Phys 1995;78:460.
[26] Jiang EY, Plamer RA, Barr NE, Morosoff N. Appl Spectrosc 1997;51:1238.
[27] Adams MJ, Kirkbright GF. Analyst 1977;102:281.
[28] Adams MJ, Kirkbright GF. Analyst 1977;102:281.
[29] Jones RW, McClelland JF. Appl Spectrsoc 1996;50:1258.
[30] Mandelis A, Teng YC, Royce BS. J Appl Phys 1979;50:7138.